Competitive Adsorption of Arsenate and Arsenite on Oxides and Clay Minerals

Sabine Goldberg*

ABSTRACT

Arsenic adsorption on amorphous Al and Fe oxides and the clay minerals, kaolinite, montmorillonite, and illite was investigated as a function of solution pH and As redox state, i.e., arsenite [As(III)] and arsenate [As(V)]. Arsenic adsorption experiments were carried out in batch systems to determine adsorption envelopes, amount of As(III), As(V), or both adsorbed as a function of solution pH per fixed total As concentration of 20 μ*M* As. Arsenate adsorption on oxides and clays was maximal at low pH and decreased with increasing pH above pH 9 for Al oxide, pH 7 for Fe oxide and pH 5 for clays. Arsenite adsorption exhibited parabolic behavior with an adsorption maximum around pH 8.5 for all materials. There was no competitive effect of the presence of equimolar arsenite on arsenate adsorption. The competitive effect of equimolar arsenate on arsenite adsorption was small and apparent only on kaolinite and illite in the pH range 6.5 to 9. The constant capacitance model was able to fit the arsenate and arsenite adsorption envelopes to obtain values of the intrinsic As surface complexation constants. These intrinsic surface complexation constants were then used in the model to predict competitive arsenate and arsenite adsorption from solutions containing equimolar As(III) and As(V) concentrations. The constant capacitance model was able to predict As adsorption from mixed As(III)-As(V) solutions in systems where there was no competitive effect.

Arsenic is a toxic trace element for animals including humans. Mineral dissolution, use of arsenical pesticides, disposal of fly ash, mine drainage, and geothermal discharge elevate concentrations of As in soils and waters. Agricultural drainage waters from some soils especially in arid regions are elevated in As concentration. Adsorption reactions on soil mineral surfaces potentially attenuate toxic soil solution As concentrations reducing contamination to groundwaters. Federal water quality standards had considered As concentrations in excess of 0.667 μmol L^{-1} (50 ppb) to be hazardous to the welfare of humans and domestic animals (USEPA, 1991). The U.S. Environmental Protection Agency (USEPA) issued a new standard for As in drinking water of 0.133. μmol L^{-1} (10 ppb) on 31 Oct. 2001 (USEPA, 2001).

Of the two inorganic redox states of As, the As(III) redox state is more acutely toxic than the As(V) redox state (Penrose, 1974). At natural pHs arsenite exists in solution as H_3AsO_3 and $H_2AsO_3^-$, since the pK_a values for arsenious acid are high, $pK_a^1 = 9.2$ and $pK_a^2 = 12.7$. Arsenate is present as $H_2AsO_4^-$ and $HAsO_4^{2-}$ since the pK_a values for arsenic acid are $pK_a^1 = 2.3$, $pK_a^2 = 6.8$, and $pK_a^3 = 11.6$. Because the kinetics of As redox transformations are relatively slow, both oxidation states are often found in soils regardless of the redox conditions (Masscheleyn et al., 1991). The mobility of As is a function of its oxidation state with arsenite exhibiting greater mobility through sand columns than arsenate (Gulens et al., 1979). However, under high pH conditions arsenite is more strongly bound to soil components than arsenate (Manning and Goldberg, 1997a; Raven et al., 1998; Jain and Loeppert, 2000).

Arsenic adsorption is significantly positively correlated with Al and Fe oxide and clay content of soils (Elkhatib et al., 1984a,b; Sakata, 1987; Wauchope, 1975; Livesey and Huang, 1981). Adsorption studies of arsenite and arsenate have used a wide range of adsorbents including oxides, clay minerals, and whole soils. Inorganic constituents of soils that adsorb significant amounts of As are Al and Fe oxides, clay minerals, and carbonates. Arsenate adsorption on amorphous Fe hydroxide (Pierce and Moore, 1982), goethite, gibbsite (Hingston et al., 1971; Manning and Goldberg, 1996a), hematite (Xu et al., 1988), amorphous Al hydroxide (Anderson et al., 1976), alumina (Gupta and Chen, 1978), kaolinite, montmorillonite (Frost and Griffin, 1977; Goldberg and Glaubig, 1988; Xu et al., 1988), and illite (Manning and Goldberg, 1996b) increased at low pH, exhibited maxima in the pH range 3 to 7, and decreased at high pH. Somewhat similar behavior was found for arsenite adsorption on amorphous Fe hydroxide (Pierce and Moore, 1980, 1982), amorphous Al oxide (Manning and Goldberg, 1997b), and alumina (Gupta and Chen, 1978) where adsorption increased at low pH, exhibited a peak in the pH range 7 to 8, and decreased at high pH. Arsenite adsorption on the clay minerals kaolinite, montmorillonite, and illite increased up to pH 9 (Manning and Goldberg, 1997b). Arsenate adsorption was greater than arsenite adsorption on alumina (Gupta and Chen, 1978), amorphous Fe hydroxide (Pierce and Moore, 1982), kaolinite, and montmorillonite (Frost and Griffin, 1977). At pH values above 7, arsenite adsorption was often greater than arsenate adsorption, as observed on amorphous Fe oxide (Jain and Loeppert, 2000; Goldberg and Johnston, 2001).

Accurate description of As adsorption behavior in natural systems requires determination of the bonding mechanism of As anions on mineral surfaces. Insight into anion adsorption mechanisms can be provided by both macroscopic (point of zero charge [PZC] shifts and ionic strength effects) and microscopic (spectroscopic) experimental methods. Electrophoretic mobility (EM) measures movement of charged particles in response to an applied electric field such that zero EM indicates the PZC of the particle. Shifts in PZC and reversals of EM with increasing ion concentration can be used as

S. Goldberg, George E. Brown Jr., Salinity Laboratory, 450 W. Big Springs Road, Riverside, CA 92507. Contribution from the George E. Brown Jr., Salinity Laboratory. Received 19 Feb. 2001. *Corresponding author (sgoldberg@ussl.ars.usda.gov).

Published in Soil Sci. Soc. Am. J. 66:413–421 (2002).

Abbreviations: EM, electrophoretic mobility; EXAFS, x-ray absorption fine structure; FTIR, Fourier transform infrared spectroscopy; PZC, point of zero charge.

evidence of strong specific ion adsorption and inner-sphere surface complex formation (Hunter, 1981).

Shifts in PZC were found upon arsenate (Hsia et al., 1994; Suarez et al., 1998; Goldberg and Johnston, 2001) and arsenite adsorption on amorphous Fe oxide (Pierce and Moore, 1980; Suarez et al., 1998) and arsenate adsorption on alumina (Ghosh and Yuan, 1987) and amorphous Al oxide (Anderson et al., 1976; Goldberg and Johnston, 2001). Arsenite adsorption on amorphous Al oxide did not produce shifts in PZC indicating the formation of an outer-sphere surface complex or an inner-sphere surface complex that did not produce a change in surface charge (Goldberg and Johnston, 2001).

Ions that form outer-sphere surface complexes show decreasing adsorption with increasing solution ionic strength, while ions that form inner-sphere surface complexes show little ionic strength dependence or show increasing adsorption with increasing solution ionic strength (McBride, 1997). Arsenate adsorption on amorphous Fe oxide (Hsia et al., 1994) and Al oxide (Goldberg and Johnston, 2001) and arsenite adsorption on amorphous Al oxide (Manning and Goldberg, 1997b) showed very little ionic strength dependence as a function of solution pH, suggesting an inner-sphere adsorption mechanism; while arsenite adsorption on amorphous Al and Fe oxide showed decreasing adsorption with increasing ionic strength indicative of an outer-sphere adsorption mechanism (Goldberg and Johnston, 2001). The apparent discrepancy between the studies can be explained. In the ionic strength range of 0.02 to 0.1 *M* there was little ionic strength dependence of As adsorption in both the study of Manning and Goldberg (1997b) and Goldberg and Johnston (2001). Ionic strength dependence became obvious in the range of 0.1 to 1.0 *M* (Goldberg and Johnston, 2001), a range not studied by Manning and Goldberg (1997b). Since ionic strength effects are more apparent in arsenite sorption studies, it is generally held that arsenite is more weakly bound than arsenate.

Spectroscopic techniques provide direct experimental observation of ion adsorption mechanisms. Arsenate was observed to form inner-sphere bidentate surface complexes on goethite using infrared (Lumsdon et al., 1984), Fourier Transform infrared (FTIR) (Sun and Doner, 1996), and x-ray absorption fine structure (EXAFS) spectroscopy (Waychunas et al., 1993; Fendorf et al., 1997). Inner-sphere surface complexes of arsenate were also observed on amorphous Fe oxide using FTIR (Suarez et al., 1998) and Raman spectroscopy (Goldberg and Johnston, 2001). Arsenite also formed inner-sphere surface complexes on goethite as observed with FTIR (Sun and Doner, 1996) and EXAFS spectroscopy (Manning et al., 1998). Adsorption of arsenate on amorphous Al oxide was found to occur as inner-sphere surface complexes using FTIR spectroscopy (Goldberg and Johnston, 2001). Arsenite surface species were observed on amorphous Al oxide using attenuated total reflectance (ATR)-FTIR spectroscopy (Suarez et al., 1998). Fourier Transform infrared analysis of KBr pellets found no discernible surface features that could be attributed to arsenite adsorbed onto amorphous Al oxide suggestive of an outer-sphere adsorption mechanism (Goldberg and Johnston, 2001).

The presence of competing anions reduced the amount of As adsorption on reference minerals. Arsenate adsorption on amorphous Fe oxide (Jain and Loeppert, 2000), goethite, gibbsite (Hingston et al., 1971; Manning and Goldberg, 1996a), kaolinite, montmorillonite, and illite (Manning and Goldberg, 1996b) was significantly reduced in the presence of competing phosphate concentrations. Arsenite adsorption by amorphous Fe oxide was also reduced in the presence of competing phosphate concentrations although some sites exhibited considerably higher selectivity for arsenite than for phosphate (Jain and Loeppert, 2000). Competitive effects of sulfate concentrations on arsenate adsorption on amorphous Fe oxide were minor (Wilkie and Hering, 1996; Jain and Loeppert, 2000). Arsenate adsorption on alumina (Xu et al., 1988) and arsenite adsorption on amorphous Fe oxide (Wilkie and Hering, 1996; Jain and Loeppert, 2000) were reduced by competing sulfate concentrations, although to a lesser degree than by competing phosphate concentrations. The competitive effect of molybdate on arsenate adsorption on goethite, gibbsite (Manning and Goldberg, 1996a), kaolinite, montmorillonite, and illite (Manning and Goldberg, 1996b) was only significant at pH values below 5. The competitive effect of arsenate on arsenite adsorption by amorphous Fe oxide at low As concentration was more pronounced than the effect of arsenite on arsenate adsorption (Jain and Loeppert, 2000). Competitive effects of As redox states on adsorption have not yet been studied on Al oxide and clay minerals.

Surface complexation models, such as the constant capacitance model, are chemical models used to describe ion adsorption on oxides and clay minerals. The constant capacitance model was able to describe arsenate and arsenite adsorption on amorphous Al and Fe oxide (Manning and Goldberg, 1997b; Goldberg and Johnston, 2001), goethite, gibbsite (Goldberg, 1986; Manning and Goldberg, 1996a), kaolinite, montmorillonite, and illite (Goldberg and Glaubig, 1988; Manning and Goldberg, 1996b). Prediction of binary competitive arsenate systems using the single ion surface complexation model parameters has met with limited success. Model predictions generally described the shape of the adsorption curves qualitatively but not quantitatively (Goldberg, 1985; Manning and Goldberg, 1996a, b). This study had the following objectives: (i) to determine arsenate and arsenite adsorption on amorphous Al and Fe oxide and the clay minerals kaolinite, montmorillonite, and illite as a function of solution pH in the presence or absence of the competing As redox state; (ii) to evaluate the ability of the constant capacitance model to fit arsenate and arsenite adsorption on these surfaces in single-ion systems; and (iii) to evaluate the ability of the model to predict arsenate and arsenite adsorption in competitive binary systems using the parameters obtained by fitting the single-ion systems.

MATERIALS AND METHODS

Arsenic adsorption behavior as a function of solution pH was studied on amorphous Al and Fe oxides and clay minerals. Amorphous Al and Fe oxide were synthesized using the method of Sims and Bingham (1968). Samples of kaolinite

(KGa-2), montmorillonite (SAz-1), and illite (IMt-2) were obtained from the Clay Minerals Society Source Clay Repository (University of Missouri, Columbia, MO). The kaolinite and montmorillonite were used without pretreatment; while the illite was ground to pass a 0.05-mm sieve. X-ray diffraction analyses verified that the oxides were amorphous and contained no trace impurities. Trace impurities in the clays were determined by x-ray diffraction using both oriented slides and random powder mounts. The kaolinite sample contained traces of vermiculite and feldspar, the montmorillonite contained traces of mica, and the illite was x-ray pure.

Surface areas for the oxides were obtained from water vapor adsorption using a combination FTIR/gravimetric apparatus (Xu et al., 2000). Surface areas of the clay minerals were determined using single-point Brunauer-Emmett-Teller (BET) N_2 adsorption isotherms obtained with a Quantasorb Jr. surface area analyzer (Quantachrome Corp., Syosset, NY). Extractable-Mn content of the clay minerals was determined using the method of Chao (1972) and found to be undetectable, 0.035, and 0.015% for kaolinite, montmorillonite, and illite, respectively.

Adsorption experiments were carried out in batch systems to determine As adsorption envelopes (amount of As adsorbed as a function of solution pH per fixed total As concentration). Samples of adsorbent were added to 250-ml centrifuge bottles or 50-ml polypropylene centrifuge tubes and equilibrated with aliquots of a 0.01 *M* NaCl solution by shaking for 2 h on a reciprocating shaker at 22.5 ± 0.08°C. Solid suspension density was 0.5 g L^{-1} for Fe oxide, 1.0 g L^{-1} for Al oxide, and 40 g L^{-1} for the clay minerals. The equilibrating solutions contained 20 μ*M* As from $Na_2HAsO_4{\cdot}7H_2O$, $NaAsO_2$, or both, and had been adjusted to the desired pH values using 0.49 *M* HCl or NaOH additions that changed the total volume by ≤2%. Arsenic additions were chosen to not exceed As concentrations found in drainage and well waters of the San Joaquin Valley of California. After reaction the samples were centrifuged at a relative centrifugal force of 7800 × *g* for 20 min. The decantates were analyzed for pH, filtered through 0.45-μm cellulose nitrate membrane filters, and analyzed directly for As(V) and As(III) concentrations using high-performance liquid chromatography coupled with hydride generation atomic absorption spectrometry as described by Manning and Martens (1997).

The constant capacitance model (Stumm et al., 1980) was used to describe arsenate and arsenite adsorption behavior on the adsorbents as a function of solution pH. The computer program FITEQL, Version 3.2 (Herbelin and Westall, 1996) was used to fit intrinsic As surface complexation constants to the experimental adsorption data. In the constant capacitance model, the protonation and dissociation reactions for the surface functional group, *X*OH (where *X*OH represents a reactive surface hydroxyl bound to a metal ion, X [Al or Fe] in the oxide mineral or an aluminol group on the clay particle edge) are defined as:

$$XOH_{(s)} + H^+_{(aq)} \rightleftharpoons XOH^+_{2(s)} \quad [1]$$

$$XOH_{(s)} \rightleftharpoons XO^-_{(s)} + H^+_{(aq)} \quad [2]$$

The constant capacitance model assumes that all surface complexes are inner-sphere. Therefore, the surface complexation reactions for arsenate adsorption:

$$XOH_{(s)} + H_3AsO_{4(aq)} \rightleftharpoons XHAsO^-_{4(s)} + H^+_{(aq)} + H_2O \quad [3]$$

$$XOH_{(s)} + H_3AsO_{4(aq)} \rightleftharpoons XAsO^{2-}_{4(s)} + 2H^+_{(aq)} + H_2O \quad [4]$$

and arsenite adsorption are defined as:

$$XOH_{(s)} + H_3AsO_{3(aq)} \rightleftharpoons XH_2AsO_{3(s)} + H_2O \quad [5]$$

$$XOH_{(s)} + H_3AsO_{3(aq)} \rightleftharpoons XHAsO^-_{3(s)} + H^+_{(aq)} + H_2O \quad [6]$$

By convention surface complexation reactions in the constant capacitance model are written starting with the completely undissociated acids. The model application contains the speciation reactions for solution As. These surface configurations were chosen because they correspond to the dominant solution As species in the pH range investigated. The unprotonated arsenate species XH_2AsO_4 was considered and found to be insignificant during model optimization. Monodentate surface species were chosen, in agreement with the FTIR, PZC, and titration results of Suarez et al. (1998) for arsenate and arsenite adsorption on amorphous Al and Fe oxides.

The intrinsic equilibrium constants for the protonation and dissociation reactions of the surface functional group are:

$$K_+(\text{int}) = \frac{[XOH^+_2]}{[XOH][H^+]} \exp(F\psi/RT) \quad [7]$$

$$K_-(\text{int}) = \frac{[XO^-][H^+]}{[XOH]} \exp(-F\psi/RT) \quad [8]$$

where F is the Faraday constant (C mol_c^{-1}), ψ is the surface potential (v), R is the molar gas constant (J mol^{-1} K^{-1}), T is the absolute temperature (K), and square brackets represent concentrations (mol L^{-1}). The intrinsic equilibrium constants for the arsenate surface complexation are:

$$K^2_{As(V)}(\text{int}) = \frac{[XHAsO^-_4][H^+]}{[XOH][H_3AsO_4]} \exp(-F\psi/RT) \quad [9]$$

$$K^3_{As(V)}(\text{int}) = \frac{[XAsO^{2-}_4][H^+]^2}{[XOH][H_3AsO_4]} \exp(-2F\psi/RT) \quad [10]$$

and the arsenite surface complexation constants are:

$$K^1_{As(III)}(\text{int}) = \frac{[XH_2AsO_3]}{[XOH][H_3AsO_3]} \quad [11]$$

$$K^2_{As(III)}(\text{int}) = \frac{[XHAsO^-_3][H^+]}{[XOH][H_3AsO_3]} \exp(-F\psi/RT) \quad [12]$$

The mass balance expression for the surface functional group is:

$$[XOH]_T = [XOH] + [XOH^+_2] + [XO^-] + [XHAsO^-_4] + [XAsO^{2-}_4] + [XH_2AsO_3] + [XHAsO^-_3] \quad [13]$$

where $[XOH]_T$ is related to the surface site density, N_s, by the following equation:

$$[XOH]_T = \frac{S_A\ C_p\ 10^{18}}{N_A} N_s \quad [14]$$

where S_A is the surface area (m^2 g^{-1}), C_p is the solid suspension density (g L^{-1}), N_A is Avogadro's number, and N_s has units of sites nm^{-2}.

The charge balance expression is:

$$\sigma = [XOH^+_2] - [XO^-] - [XHAsO^-_4] - 2[XAsO^{2-}_4] - [XHAsO^-_3] \quad [15]$$

where σ represents the surface charge (mol_c L^{-1}). The relationship between surface charge and surface potential is:

$$\sigma = \frac{CS_A\ C_p}{F} \psi \quad [16]$$

where C is the capacitance (F m^{-2}).

The surface-site density was set at a value of 2.31 sites

nm^{-2} as recommended by Davis and Kent (1990) for natural materials. Use of a consistent site density value for all materials is critical to allow standardization of parameters for natural systems. Numerical values of the intrinsic protonation constant, K_+(int), and the intrinsic dissociation constant, K_-(int), were averages of experimental values compiled from the literature for Al and Fe oxides (Goldberg and Sposito, 1984). The intrinsic protonation-dissociation constants were fixed at log K_+(int) = 7.31, log K_-(int) = −8.80 for amorphous Fe oxide and log K_+(int) = 7.38, log K_-(int) = −9.09 for amorphous Al oxide and kaolinite and illite. To obtain an acceptable model fit to the montmorillonite adsorption data it was necessary to optimize the protonation-dissociation constants along with the As surface complexation constants. This is likely because of the preponderance of permanent negative charge sites and resultant low PZC of the montmorillonite mineral. The capacitance was fixed at $C = 1.06$ F m^{-2} for all materials as had been done in previous constant capacitance modeling of arsenate adsorption on amorphous Al and Fe oxide (Goldberg, 1986; Manning and Goldberg, 1997b; Goldberg and Johnston, 2001) and considered optimum for Al oxide by Westall and Hohl (1980).

RESULTS AND DISCUSSION

Arsenate and arsenite adsorption as a function of solution pH on all materials is indicated in Fig. 1 through 5. Direct analytical determination of both oxidation states verified that neither oxidation of arsenite to arsenate nor reduction of arsenate to arsenite was occurring in the oxide systems or in the presence of kaolinite or illite. In the montmorillonite system oxidation of arsenite to arsenate was found. In the pH range 5 to 9, conversion of arsenite to arsenate was <5% of total As added. Outside this range, oxidation of arsenite ranged from 12% of total As added at pH 10.9 to 43% at pH 3.3. Because of the oxidation, accurate assessment of arsenite adsorption was not possible in these pH ranges since it was impossible to determine whether oxidation of arsenite had taken place on the solid surface or in aqueous solution. Arsenite oxidation on montmorillonite was likely due to the increased extractable-Mn content of this clay. Continued reaction of IMt-2 illite for 16 h has been found to result in some oxidation of arsenite (Manning and Goldberg, 1997b) not seen in our 2-h study.

Arsenate adsorption on amorphous Al oxide, as represented in Fig. 1a, showed 100% adsorption from pH 3 to 9 and then decreased with additional increases in solution pH. Arsenite adsorption on Al oxide exhibited a parabolic adsorption curve (Fig. 1b); adsorption increased with increasing solution pH from pH 3 to 8 and then decreased with increasing pH from pH 8 to 10.5. Arsenate adsorption on amorphous Fe oxide shows 100% adsorption from pH 3 to 7 and decreasing adsorption with increasing pH above pH 8 (Fig. 2a). In contrast to its behavior on Al oxide, arsenite adsorption on Fe oxide was virtually 100% throughout the entire pH range investigated, pH 2.5 to 10.5 (Fig. 2b). Thus it appears that amorphous Fe oxide had a greater affinity for adsorption of arsenite than amorphous Al oxide.

Adsorption behavior on the clay minerals was very similar to that on the oxides with respect to the shape of the adsorption envelopes, showing adsorption maxima for arsenate around pH 5 (Fig. 3a, 4a, and 5a) and adsorption maxima for arsenite at pH 8 to 9 (Fig. 3b, 4b, and 5b). Contrary to its behavior on oxides (Fig. 1a and 2a), arsenate adsorption on the clays increased with increasing solution pH from pH 3 to 5 and decreased with increasing solution pH from pH 5 to 9 (Fig. 3a, 4a, and 5a). The renewed increase in arsenate adsorption

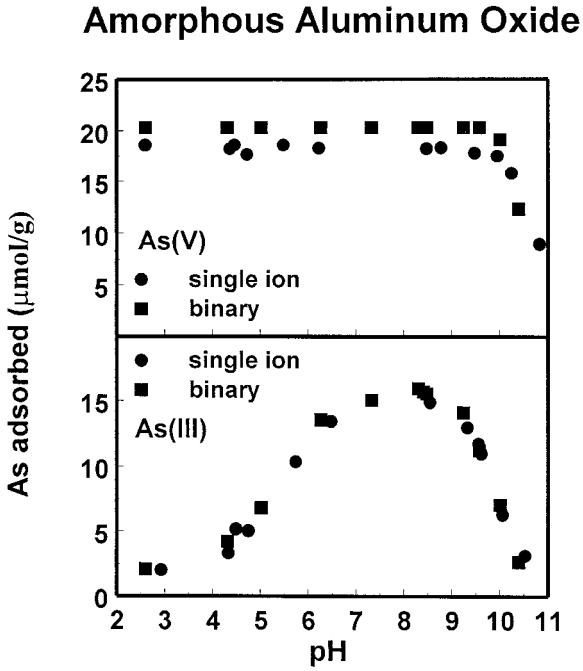

Fig. 1. Arsenic adsorption on amorphous Al oxide as a function of pH and As redox state: (a) arsenate; (b) arsenite. Single ion systems: As_T = 20 μ*M*. Binary systems: $As(III)_T = As(V)_T$ = 20 μ*M*. Suspension density: 1 g L^{-1}.

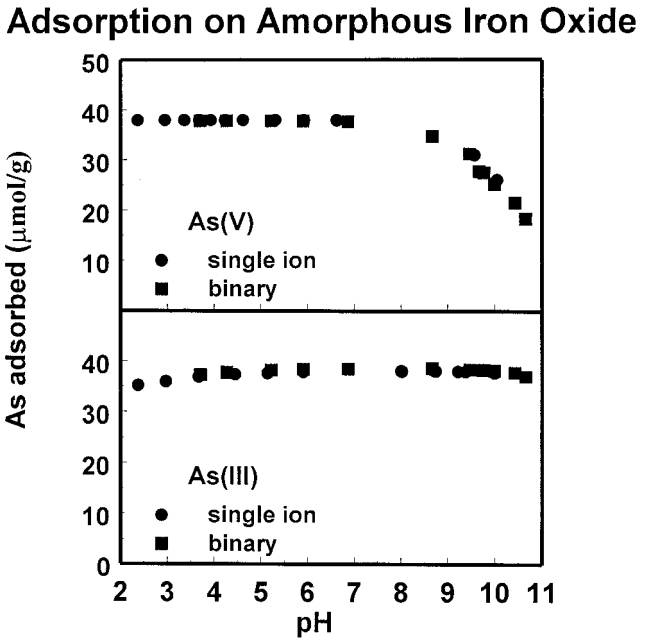

Fig. 2. Arsenic adsorption on amorphous Fe oxide as a function of pH and As redox state: (a) arsenate; (b) arsenite. Single ion systems: As_T = 20 μ*M*. Binary systems: $As(III)_T = As(V)_T$ = 20 μ*M*. Suspension density: 0.5 g L^{-1}.

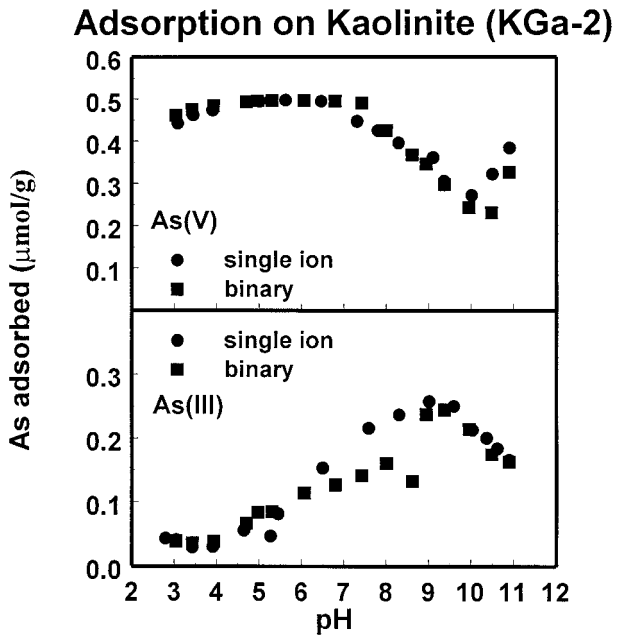

Fig. 3. Arsenic adsorption on kaolinite as a function of pH and As redox state: (a) arsenate; (b) arsenite. Single-ion systems: As_T = 20 μ*M*. Binary systems: $As(III)_T = As(V)_T$ = 20 μ*M*. Suspension density: 40 g L^{-1}.

observed when pH increased above pH 9 was most likely an artifact resulting from dissolution of the clay minerals at elevated pH. Adsorption affinity for As of the clay minerals was less than the adsorption affinity of the oxides. Adsorption of As at 100% was only reached on kaolinite by arsenate around pH 5. For all other clay systems adsorption was significantly below 100%, especially for the arsenite systems.

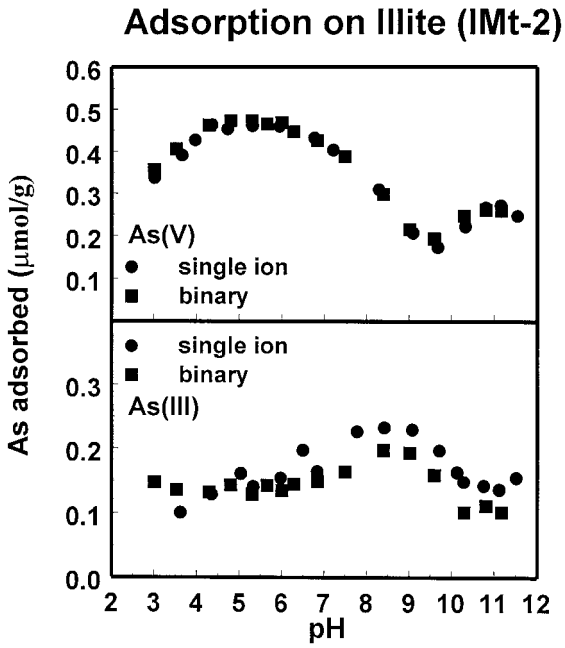

Fig. 4. Arsenic adsorption on illite as a function of pH and As redox state: (a) arsenate; (b) arsenite. Single-ion systems: As_T = 20 μ*M*. Binary systems: $As(III)_T = As(V)_T$ = 20 μ*M*. Suspension density: 40 g L^{-1}.

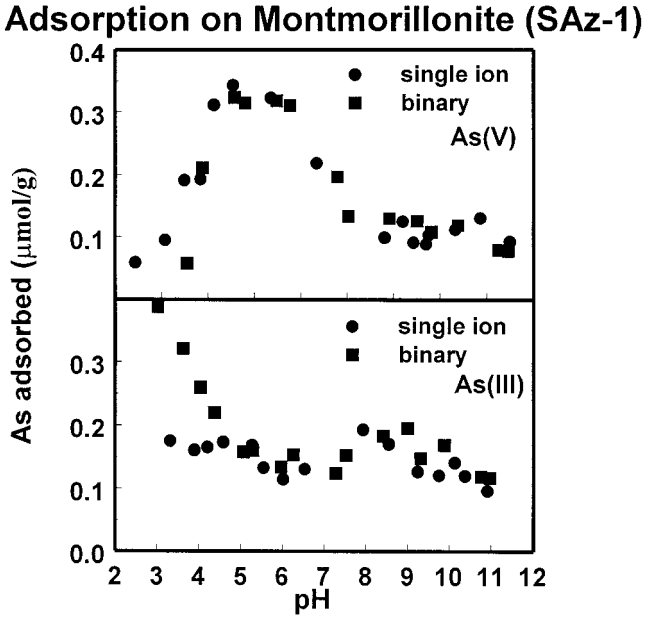

Fig. 5. Arsenic adsorption on montmorillonite as a function of pH and As redox state: (a) arsenate; (b) arsenite. Single-ion systems: As_T = 20 μ*M*. Binary systems: $As(III)_T = As(V)_T$ = 20 μ*M*. Suspension density: 40 g L^{-1}.

The competitive effect of the presence of equimolar concentrations of the both As redox states is also shown in Fig. 1 through 5. In the oxide systems there was no evidence of any competitive effect (Fig. 1 and 2). The discrepancy in arsenate adsorption on Al oxide between the binary and the single ion system was the result of

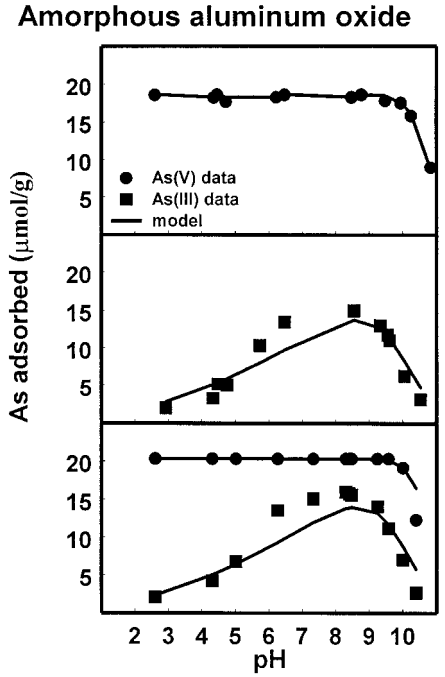

Fig. 6. Application of the constant capacitance model to As adsorption on amorphous Al oxide as a function of solution pH: (a) fit to arsenate adsorption in single-ion system; (b) fit to arsenite adsorption in single ion system; (c) prediction of competitive arsenate and arsenite adsorption in binary system. Model results are indicated by solid lines.

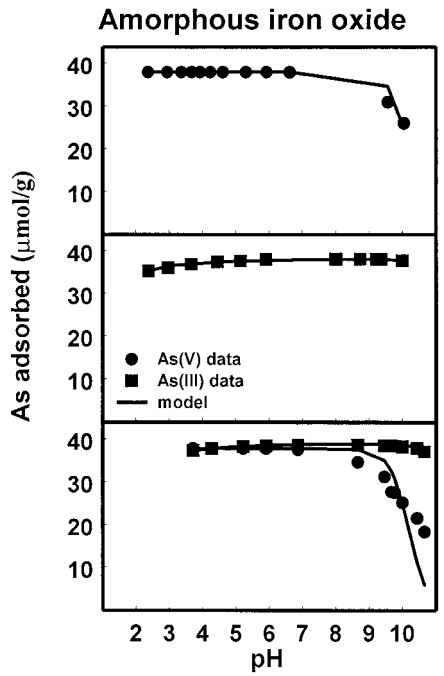

Fig. 7. Application of the constant capacitance model to As adsorption on amorphous Fe oxide as a function of solution pH: (a) fit to arsenate adsorption in single-ion system; (b) fit to arsenite adsorption in single-ion system; (c) prediction of competitive arsenate and arsenite adsorption in binary system. Model results are indicated by solid lines.

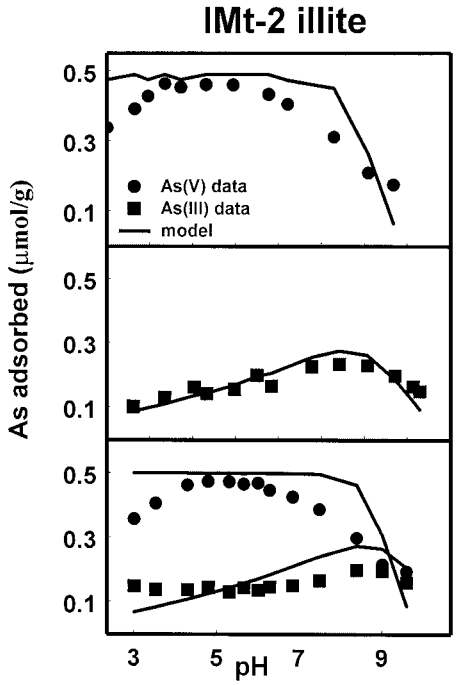

Fig. 9. Application of the constant capacitance model to As adsorption on IMt-2 illite as a function of solution pH: (a) fit to arsenate adsorption in single ion system; (b) fit to arsenite adsorption in single-ion system; (c) prediction of competitive arsenate and arsenite adsorption in binary system. Model results are indicated by solid lines.

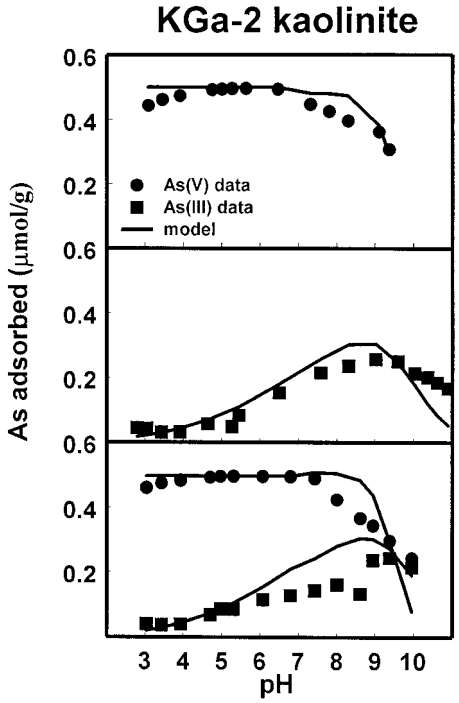

Fig. 8. Application of the constant capacitance model to As adsorption on KGa-2 kaolinite as a function of solution pH: (a) fit to arsenate adsorption in single ion system; (b) fit to arsenite adsorption in single ion system; (c) prediction of competitive arsenate and arsenite adsorption in binary system. Model results are indicated by solid lines.

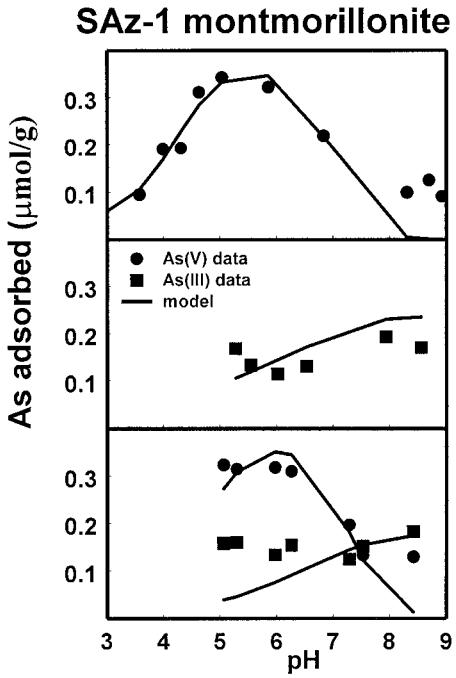

Fig. 10. Application of the constant capacitance model to As adsorption on SAz-1 montmorillonite as a function of solution pH: (a) fit to arsenate adsorption in single ion system; (b) fit to arsenite adsorption in single ion system; (c) prediction of competitive arsenate and arsenite adsorption in binary system. Model results are indicated by solid lines.

Table 1. Modeling parameters for the constant capacitance model.

Parameter	am†-Al-oxide	am-Fe-oxide	KGa-2 kaolinite	IMt-2 illite	SAz-1 montmorillonite
Surface area, $m^2\ g^{-1}$	660	350	21.6	22.6	68.9
Site density, sites nm^{-2}	2.31‡	2.31‡	2.31‡	2.31‡	2.31‡
Capacitance, $F\ m^{-2}$	1.06§	1.06§	1.06§	1.06§	1.06§
Protonation constant, $logK_+(int)$	7.38¶	7.31¶	7.38¶	7.38¶	1.89
Dissociation constant, $logK_-(int)$	−9.09¶	−8.80¶	−9.09¶	−9.09¶	−6.29
Arsenic constants					
$logK^2_{As(V)}(int)$	2.51				−4.52
$logK^3_{As(V)}(int)$	−2.45	−2.35	−4.69	−5.21	
$logK^1_{As(III)}(int)$	2.20	4.68		2.12	1.19
$logK^2_{As(III)}(int)$	−5.17	−2.27	−5.43	−5.66	−3.92

† Amorphous.
‡ From Davis and Kent (1990).
§ From Goldberg (1986).
¶ From Goldberg and Sposito (1984).

differences in amount of total As added; both systems exhibited 100% adsorption from pH 3 to 9. There was no apparent competitive effect of arsenite on arsenate adsorption for the clay minerals (Fig. 3a, 4a, and 5a). Differences below pH 4 and above pH 10 should be ignored because of the likelihood of significant clay dissolution at these pH values. The data points for arsenate adsorption on montmorillonite below pH 3.5 could also be artificially low because of significant oxidation of arsenite occurring at these pH values. A competitive effect of the presence of arsenate on adsorption of arsenite was observed on kaolinite (Fig. 3b) and illite (Fig. 4b) in the intermediate pH range 6.5 to 9. No comparable competitive effect was observed for montmorillonite in the pH range 5 to 9 (Fig. 5b); the apparent increase in arsenite adsorption below pH 5 resulted because of the oxidation of arsenite to arsenate. The minor competitive effects in the systems studied were not surprising considering the small, environmentally realistic concentrations of As that were added, leading to surface concentrations that were far from site saturation (3.8×10^{-2} μmol m^{-2} for As(V) and 2.3×10^{-2} μmol m^{-2} for As(III) on amorphous Al oxide and 1.1×10^{-2} μmol m^{-2} for As(V) and 1.0×10^{-2} μmol m^{-2} for As(III) on amorphous Fe oxide). However, as has been shown by Benjamin and Leckie (1981) for metal adsorption on oxides, competitive effects can be observed at low surface coverage when site heterogeneity is present. Previous competitive adsorption studies of arsenate and phosphate on goethite and gibbsite have been conducted under conditions of site saturation (e.g., Hingston et al., 1971, 1.3 μmol P m^{-2}). The only previous study of arsenate-arsenite competitive adsorption was carried out at sufficiently high loading rates that precipitation rather than adsorption may have been occurring (Jain and Loeppert, 2000; Jain et al., 1999a,b; Stanforth, 1999).

The ability of the constant capacitance model to describe arsenate and arsenite adsorption on oxides and clay minerals is depicted in Fig. 6 through 10. Surface complexation model parameters used to obtain the model fits are indicated in Table 1. The fit of the model to arsenate adsorption on oxides and on montmorillonite below pH 8 was excellent (Fig. 6a, 7a, and 10a, respectively). For arsenate on kaolinite and illite the model fit overestimated adsorption below pH 4 and around pH 8 (Fig. 8a and 9a, respectively). The overprediction at low pH is not considered significant since dissolution of the clay mineral would be expected. It is not clear why the model overestimated adsorption at intermediate pH value.

Arsenite adsorption on amorphous Fe oxide and illite was fit quantitatively by the constant capacitance model (Fig. 7b and 9b). Fit of the model to arsenite adsorption on amorphous Al oxide and kaolinite showed some deviations from experimental values in the pH range 7 to 9; underprediction for Al oxide (Fig. 6b) and overprediction for kaolinite (Fig. 8b). It was difficult to judge the ability of the model to describe arsenite adsorption on montmorillonite since only a small number of data points were available in the pH range 5 to 9 where reduction reactions are insignificant (Fig. 10b). The apparent ability of the model to describe adsorption of both arsenite and arsenate indicates that the inner-sphere adsorption mechanism assumed by the constant capacitance model is the appropriate adsorption mechanism for both oxidation states. The ability of the surface complexation model to predict competitive adsorption of arsenate and arsenite from model parameters obtained from the fitting of single ion systems is indicated in Fig. 6c, 7c, 8c, 9c, and 10c. In the oxide systems where there was no competitive effect, the model predictions of the binary systems were comparable with the quality of the fit to the single ion experimental data (Fig. 6c and 7c). For montmorillonite the predictive ability of the model to describe arsenate adsorption in the presence of arsenite was good; evaluation of the model capability for predicting arsenite adsorption was not possible because of the small number of data points that were used to fit the arsenite single-ion system. In the kaolinite (Fig. 8c) and illite (Fig. 9c) systems the model predictions for the binary system were unable to describe the competitive effect of arsenate on arsenite adsorption occurring in the pH range 7 to 9. Since the competitive effect is not a result of site saturation, it is clear that the model is overly simplistic in its present form. Appropriate modifications to include the effect of site heterogeneity are needed and would be expected to lead to more accurate description of competitive ion adsorption.

ACKNOWLEDGMENTS

Gratitude is expressed to Mr. H. Forster for technical assistance and to Mr. S.-L. Wang and Dr. C.T. Johnston for conducting the water adsorption surface area measurements.

REFERENCES

Anderson, M.A., J.F. Ferguson, and J. Gavis. 1976. Arsenate adsorption on amorphous aluminum hydroxide. J. Colloid Interface Sci. 54:391–399.

Benjamin, M.M., and J.O. Leckie. 1981. Multiple-site adsorption of Cd, Cu, Zn, and Pb on amorphous iron oxyhydroxide. J. Colloid Interface Sci. 79:209–221.

Chao, T.T. 1972. Selective dissolution of manganese oxides from soils and sediments with acidified hydroxylamine hydrochloride. Soil Sci. Soc. Am. Proc. 36:764–768.

Davis, J.A., and D.B. Kent. 1990. Surface complexation modeling in aqueous geochemistry. Rev. Mineralogy 23:117–260.

Elkhatib, E.A., O.L. Bennett, and R.J. Wright. 1984a. Kinetics of arsenite sorption in soils. Soil Sci. Soc. Am. J. 48:758–762.

Elkhatib, E.A., O.L. Bennett, and R.J. Wright. 1984b. Arsenite sorption and desorption in soils. Soil Sci. Soc. Am. J. 48:1025–1030.

Fendorf, S., M.J. Eick, P. Grossl, and D.L. Sparks. 1997. Arsenate and chromate retention mechanisms on goethite. 1. Surface structure. Environ. Sci. Technol. 31:315–320.

Frost, R.R., and R.A. Griffin. 1977. Effect of pH on adsorption of arsenic and selenium from landfill leachate by clay minerals. Soil Sci. Soc. Am. J. 41:53–57.

Ghosh, M.M., and J.R. Yuan. 1987. Adsorption of inorganic arsenic and organoarsenicals on hydrous oxides. Environ. Prog. 6:150–157.

Goldberg, S. 1985. Chemical modeling of anion competition on goethite using the constant capacitance model. Soil Sci. Soc. Am. J. 49:851–856.

Goldberg, S. 1986. Chemical modeling of arsenate adsorption on aluminum and iron oxide minerals. Soil Sci. Soc. Am. J. 50:1154–1157.

Goldberg, S., and R.A. Glaubig. 1988. Anion sorption on a calcareous, montmorillonitic soil—Arsenic. Soil Sci. Soc. Am. J. 52:1297–1300.

Goldberg, S., and C.T. Johnston. 2001. Mechanisms of arsenic adsorption on amorphous oxides evaluated using macroscopic measurements, vibrational spectroscopy, and surface complexation modeling. J. Colloid Interface Sci. 234:204–216.

Goldberg, S., and G. Sposito. 1984. A chemical model of phosphate adsorption by soils: I. Reference oxide minerals. Soil Sci. Soc. Am. J. 48:772–778.

Gulens, J., D.R. Champ, and R.E. Jackson. 1979. Influence of redox environments on the mobility of arsenic in ground water. Am. Chem. Soc. Symp. Ser. 93:81–95.

Gupta, S.K., and K.Y. Chen. 1978. Arsenic removal by adsorption. J. Water Pollution Control Fed. 50:493–506.

Herbelin, A.L., and J.C. Westall. 1996. FITEQL: A computer program for determination of chemical equilibrium constants from experimental data. Rep. 96-01, Vers. 3.2, Dep. of Chemistry, Oregon State Univ., Corvallis, OR.

Hingston, F.J., A.M. Posner, and J.P. Quirk. 1971. Competitive adsorption of negatively charged ligands on oxide surfaces. Disc. Faraday Soc. 52:334–342.

Hsia, T.-H., S.-L. Lo, C.-F. Lin, and D.-Y. Lee. 1994. Characterization of arsenate adsorption on hydrous iron oxide using chemical and physical methods. Colloids Surf. A: Physicochem. Eng. Aspects 85:1–7.

Hunter, R.J. 1981. Zeta potential in colloid science. Academic Press, London.

Jain, A., and R.H. Loeppert. 2000. Effect of competing anions on the adsorption of arsenate and arsenite by ferrihydrite. J. Environ. Qual. 29:1422–1430.

Jain, A., K.P. Raven, and R.H. Loeppert. 1999a. Arsenite and arsenate adsorption on ferrihydrite: Surface charge reduction and net OH^- release. Environ. Sci. Technol. 33:1179–1184.

Jain, A., K.P. Raven, and R.H. Loeppert. 1999b. Response to Comment on "Arsenite and arsenate adsorption on ferrihydrite: Surface charge reduction and net OH^- release". Environ. Sci. Technol. 33:3696.

Livesey, N.T., and P.M. Huang. 1981. Adsorption of arsenate by soils and its relation to selected chemical properties and anions. Soil Sci. 131:88–94.

Lumsdon, D.G., A.R. Fraser, J.D. Russell, and N.T. Livesey. 1984. New infrared band assignments for the arsenate ion adsorbed on synthetic goethite (α-FeOOH). J. Soil Sci. 35:381–386.

Manning, B.A., S.E. Fendorf, and S. Goldberg. 1998. Surface structures and stability of arsenic(III) on goethite: Spectroscopic evidence for inner-sphere complexes. Environ. Sci. Technol. 32:2383–2388.

Manning, B.A., and S. Goldberg. 1996a. Modeling competitive adsorption of arsenate with phosphate and molybdate on oxide minerals. Soil Sci. Soc. Am. J. 60:121–131.

Manning, B.A., and S. Goldberg. 1996b. Modeling arsenate competitive adsorption on kaolinite, montmorillonite and illite. Clays Clay Miner. 44:609–623.

Manning, B.A., and S. Goldberg. 1997a. Arsenic(III) and arsenic(V) adsorption on three California soils. Soil Sci. 162:886–895.

Manning, B.A., and S. Goldberg. 1997b. Adsorption and stability of arsenic(III) at the clay mineral—Water interface. Environ. Sci. Technol. 31:2005–2011.

Manning, B.A., and D.A. Martens. 1997. Speciation of arsenic(III) and arsenic(V) in sediment extracts by high-performance liquid chromatography—Hydride generation atomic absorption spectrophotometry. Environ. Sci. Technol. 31:171–177.

Masscheleyn, P.H., R.D. Delaune, and W.H. Patrick. 1991. Effect of redox potential and pH on arsenic speciation and solubility in a contaminated soil. Environ. Sci. Technol. 25:1414–1419.

McBride, M.B. 1997. A critique of diffuse double layer models applied to colloid and surface chemistry. Clays Clay Miner. 45:598–608.

Penrose, W.R. 1974. Arsenic in the marine and aquatic environments: Analysis, occurrence, and significance. CRC Critical Reviews in Environmental Control 4:465–482.

Pierce, M.L., and C.B. Moore. 1980. Adsorption of arsenite on amorphous iron hydroxide from dilute aqueous solution. Environ. Sci. Technol. 14:214–216.

Pierce, M.L., and C.B. Moore. 1982. Adsorption of arsenite and arsenate on amorphous iron hydroxide. Water Res. 16:1247–1253.

Raven, K.P., A. Jain, and R.H. Loeppert. 1998. Arsenite and arsenate adsorption on ferrihydrite: Kinetics, equilibrium, and adsorption envelopes. Environ. Sci. Technol. 32:344–349.

Sakata, M. 1987. Relationship between adsorption of arsenic(III) and boron by soil and soil properties. Environ. Sci. Technol. 21:1126–1130.

Sims, J.T., and F.T. Bingham. 1968. Retention of boron by layer silicates, sesquioxides, and soil materials: II. Sesquioxides. Soil Sci. Soc. Am. Proc. 32:364–369.

Stanforth, R. 1999. Comment on "Arsenite and arsenate adsorption on ferrihydrite: Surface charge reduction and net OH^- release". Environ. Sci. Technol. 33:3695.

Stumm, W., R., Kummert, and L. Sigg. 1980. A ligand exchange model for the adsorption of inorganic and organic ligands at hydrous oxide interfaces. Croatica Chem. Acta 53:291–312.

Suarez, D.L., S. Goldberg, and C. Su. 1998. Evaluation of oxyanion adsorption mechanisms on oxides using FTIR spectroscopy and electrophoretic mobility. Am. Chem. Soc. Symp. Ser. 715:136–178.

Sun, X., and H.E. Doner. 1996. An investigation of arsenate and arsenite bonding structures on goethite by FTIR. Soil Sci. 161: 865–872.

United States Enivornment Protection Agency (USEPA). 1991. National primary drinking water regulations: Final rule. Federal Register. Vol. 56. No. 20. p. 3526. 30 Jan. 2001. U.S. Gov. Print Office, Washington DC.

USEPA. 2001. EPA to implement 10 ppb standard for arsenic in drinking water–EPA 815-F-01-010. 31 Oct. 2001. U.S. Gov. Print Office, Washington, DC.

Wauchope, R.D. 1975. Fixation of arsenical herbicides, phosphate, and arsenate in alluvial soils. J. Environ. Qual. 4:355–358.

Waychunas, G.A., B.A. Rea, C.C. Fuller, and J.A. Davis. 1993. Surface chemistry of ferrihydrite: Part 1. EXAFS studies of the geometry of coprecipitated and adsorbed arsenate. Geochim. Cosmochim. Acta 57:2251–2269.

Westall, J., and H. Hohl. 1980. A comparison of electrostatic models for the oxide/solution interface. Adv. Colloid Interface Sci. 12:265–294.

Wilkie, J.A., and J.G. Hering. 1996. Adsorption of arsenic onto hydrous ferric oxide: Effects of adsorbate/adsorbent ratios and co-occuring solutes. Colloids Surf. A: Physicochem. Eng. Aspects 107: 97–110.

Xu, H., B. Allard, and A. Grimvall. 1988. Influence of pH and organic substance on the adsorption of As(V) on geologic materials. Water Air Soil Pollut. 40:293–305.

Xu, W., C.T. Johnston, P. Parker, and S.F. Agnew. 2000. Infrared study of water sorption on Na-, Li-, Ca- and Mg-exchanged (SWy-1 and SAz-1) montmorillonite. Clays Clay Miner. 48:120–131.

Soil Organic Matter Characteristics as Affected by Tillage Management

G. Ding, J. M. Novak, D. Amarasiriwardena, P. G. Hunt, and B. Xing*

ABSTRACT

Soil organic matter (SOM) is of primary importance for maintaining soil productivity, and agricultural management practices may significantly influence SOM chemical properties. However, how SOM chemical characteristics change with agricultural practices is poorly understood. Therefore, in this study, we evaluated the impacts of tillage (conventional vs. conservation) management on the structural and compositional characteristics of SOM using cross-polarization magic-angle-spinning (CPMAS) and total sideband suppression (TOSS) solid-state ^{13}C nuclear magnetic resonance (NMR) and diffuse reflectance Fourier transform infrared (DRIFT) spectroscopy. We characterized both physically and chemically isolated SOM fractions from a Norfolk soil (fine-loamy, siliceous, thermic Typic Kandiudults) under long-term tillage management (20 yr). The solid-state ^{13}C NMR results indicated that humic acid (HA) from conventional tillage (CT, 0–5 cm) was less aliphatic and more aromatic than HA from conservation tillage (CnT). The aliphatic C content decreased with increasing depth (0–15 cm) for both CT and CnT treatments. The reverse trend was true for aromatic C content. Based on reactive/recalcitrant (O/R) peak ratio comparisons, HA was more reactive in the top soil (0–5 cm) under CnT than CT. Both soil organic C (SOC) and light fraction (LF) material were higher in the 0- to 5-cm soil of CnT than CT treatment. Our results show that long-term tillage management can significantly change the characteristics of both physical and chemical fractions of SOM.

Soil organic matter strongly affects soil properties such as water infiltration rate, erodibility, water holding capacity, nutrient cycling, and pesticide adsorption (Stevenson, 1994; Campbell et al., 1996; Francioso et al., 2000; Wander and Yang, 2000). It has been suggested that proper management of SOM is the heart of sustainable agriculture (Weil, 1992). Recent research has also recognized SOM as a central indicator of soil quality and health (Soil and Water Conservation Society, 1995). For example, a decline in SOM (biological oxidation or erosion) significantly reduced the N supply and resulted in a deterioration of soil physical conditions, leading to crop yield reduction (Greer et al., 1996). Therefore, it is important to maintain proper levels of SOM to sustain soil productivity.

Intensive agricultural practices change SOM characteristics greatly, generally a substantial loss of soil organic C (SOC). Soils of the southeastern United States of America, particularly sandy Coastal Plain soils, have inherently low SOC contents (typically below 1%, Hunt et al., 1982). Consequently, small changes in the SOM content are significant to the agricultural production of the region. An evaluation of tillage and crop residue management practices to rebuild SOC levels has been conducted by Hunt et al. (1996). These researchers monitored changes in SOC levels in numerous small tillage plots and found that after 9 yr of CnT, the SOC content in the top few centimeters was significantly higher than the soil under CT management. Campbell et al. (1999) reported that over an 11- to 12-yr period, increases in C storage in the 0- to 15-cm soil depth, because of adoption of no-tillage, were small (0–3 Mg ha^{-1}). Most of the differences were observed in the 0- to 7.5-cm soil depth, with little change in the 7.5 to 15 cm. However, the short and long-term influences of disturbance on C mineralization are complex and may vary depending on types of soil and plant residues (Hu et al., 1995; Franzleubbers and Arshad, 1996; Alvarez et al., 1998). The strong influence of soil management on the amount and quality of SOM was also reported by others (Janzen et al., 1992; Ismail et al., 1994; Campbell et al., 1996).

Another approach to evaluate the impact of agricultural management on SOM dynamics is to separate SOM into pools based on differences in decomposition rates (Wander et al., 1994; Wander and Traina, 1996a). Generally, those pools are conceptualized with one small pool having a relatively quick decomposition rate (i.e., active pool LF) and pools that are more recalcitrant (i.e., humus) (Stevenson, 1994). The LF is sensitive to environmental and agricultural management factors and can be used as a functional description of organic materials (Wander and Traina, 1996a). Regardless of active or recalcitrant SOM pools, structural chemistry is important for their chemical and biological activities.

Spectroscopic techniques can provide useful structural information of SOM. Diffuse reflectance Fourier transform infrared spectroscopy is considered to be one of the most sensitive infrared techniques for humic substances analysis (Niemeyer et al., 1992; Ding et al., 2000). According to Painter et al. (1985) and Niemeyer et al.

G. Ding and B. Xing, Dep. of Plant and Soil Sciences, University of Massachusetts, Amherst, MA 01003; J.M. Novak and P.G. Hunt, USDA-ARS-Coastal Plains Soil, Water, and Plant Research Center, Florence, SC 29501; D. Amarasiriwardena, School of Natural Science, Hampshire College, Amherst, MA 01002. Received 17 Jan. 2001. *Corresponding author (bx@pssci.umass.edu).

Published in Soil Sci. Soc. Am. J. 66:421–429 (2002).

Abbreviations: CnT, conservation tillage; CPMAS-NMR, cross-polarization magic-angle-spinning nuclear magnetic resonance; CT, conventional tillage; DRIFT, diffuse reflectance Fourier transform infrared spectroscopy; HA, humic acid; LF, light fraction; O/R, reactive/recalcitrant functional group ratio calculated from peak heights of DRIFT spectra; SOC, soil organic C; SOM, soil organic matter; TCN, total combustible N; TOSS, total sideband suppression.